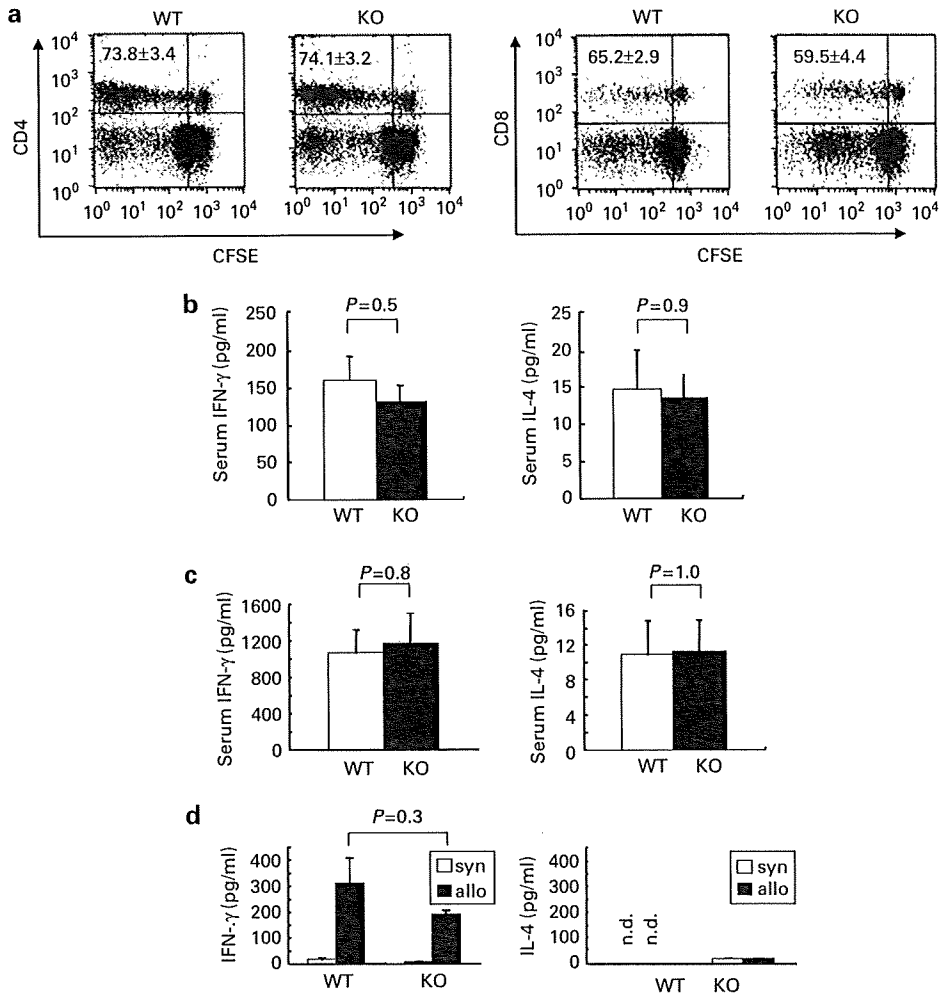

Figure 2 Proliferation and cytokine production after transplantation. (**a**) Flow cytometric analysis of CD4/CD8 proliferation *in vivo* by carboxyfluorescein diacetate succinimidyl ester (CFSE) staining. Splenocytes (SPs) (H-2^b 1×10^8) from either wild type (WT) or IL-21R knockout (KO) mice were stained with CFSE and transplanted into irradiated Balb/c mice; three days later, SPs were collected and analyzed. Donor cells were selected by gating on H-2^{d-}. The numbers at left quadrants were the percentage of dividing cells in CD4 or CD8 cells (mean ± s.e.m.). Total number of recipients analyzed was six mice in each group. (**b**) Serum cytokine concentrations at day 14 after transplantation. Balb/c recipients were transplanted with 5×10^6 IL-21R KO-BM and either 5×10^6 IL-21R KO-SP or WT-SP. Serum was sampled at day 14 after transplantation, and cytokine concentrations of IFN-γ (left panel) and IL-4 (right panel) were determined by ELISA. Total number of recipients analyzed was more than six mice in each group. (**c**) Serum cytokine concentrations at day 6 after transplantation. C57BL/6-DBA2 F1 recipients were transplanted with 1×10^8 SPs from WT or IL-21R KO mice. Serum was sampled at day 6 after transplantation, and cytokine concentrations of IFN-γ (left panel) and IL-4 (right panel) were determined by ELISA. Total number of recipients analyzed was five mice in each group. (**d**) Transplantations were carried out as in (**c**). At day 6, SPs (1×10^5) from recipients of WT-SP or IL-21R KO-SP were incubated with 30 Gy irradiated 4×10^5 SPs from C57BL/6 (syngeneic) or C57BL/6-DBA2 F1 (allogeneic) mice. After 72 h, cytokine concentrations in the supernatants were determined by ELISA. Total number of recipients analyzed was five mice in each group.

ELISA

Enzyme linked immunosorbent assay kits for cytokines, IFN-γ and IL-4 were purchased from BD Bioscience or R&D Systems. Concentrations were determined according to the manufacturer's instructions.

Statistical analysis

Kaplan–Meier plots were used to compare survival rates. The log-rank test was used to evaluate P values. The Mann–Whitney U test was used to calculate P values for the GVHD clinical score. Statistical analyses were performed using "Stat Mate ver. 6" (ATMS, Tokyo, Japan). Unless otherwise specified, all error bars in this study are s.e.m.

Results

IL-21R$^{-/-}$ SPs (KO-SP) cause attenuated GVHD with WT-BM

A well-established MHC-mismatch CD4 T cell-mediated GVHD model, C57BL/6 (H-2^b) → Balb/c (H-2^d), was used to evaluate the role for IL-21 in GVHD. BM cells and SPs were taken from donor C57BL/6 WT or IL-21R KO mice

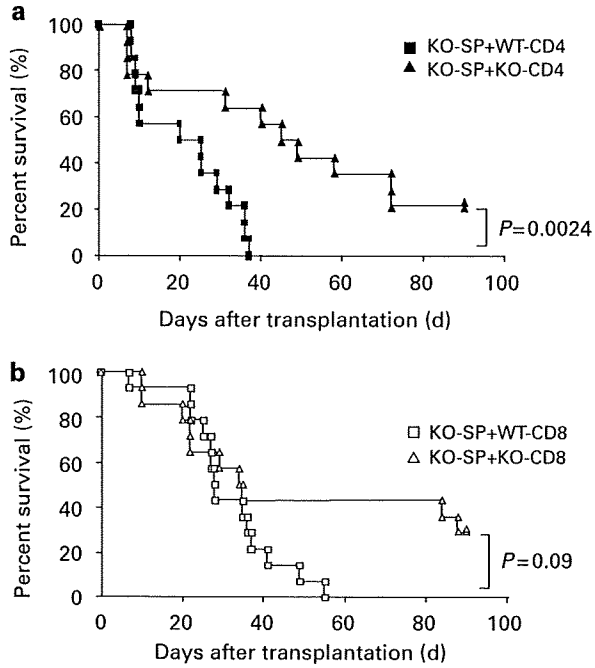

Figure 3 Effects of additional CD4 or CD8 T cells on survival. (**a**) Survival curve with addition of either wild type (WT)- or IL-21R knockout (KO)-CD4 cells. Transplantations were carried out as in Figure 1c. CD4 T cells (5×10^5) from either WT or KO mice were transplanted concomitantly with KO-BM (5×10^6) and KO-splenocyte (SP) (5×10^6). (**b**) Survival curve with addition of either WT- or IL-21R KO-CD8 cells. CD8 T cells (5×10^5) from either WT or IL-21R KO mice were transplanted with IL-21R KO-BM (5×10^6) and IL-21R KO-SP (5×10^6). The combined results of three independent experiments are shown. *P*-value was calculated by log-rank method.

and transplanted into irradiated Balb/c mice. Recipients of BM and SPs from WT mice became ill after 3–4 weeks and suffered from diarrhea, ruffled hair, a hunched posture and diminished body weight. In contrast, mice transplanted from IL-21R KO mice showed attenuated GVHD symptoms and survived longer (Figure 1a, $P=0.0003$, log-rank test). Strikingly, no mouse receiving the WT-SPs group survived more than 4 months, whereas 40% of the mice receiving the IL-21R KO SPs survived for 4 months or longer. Consistent with this, clinical GVHD scores in mice transplanted from IL-21R KO-SPs were significantly less than those in controls (Figure 1b). In both groups, approximately 85% engraftment in peripheral blood was achieved, indicating that the difference was not attributable to a difference in engraftment.

KO-SP causes attenuated GVHD when combined with KO-BM

In the preceding experiments (Figures 1a and b), we used unfractionated WT-BM, which presumably contained IL-21R-expressing T cells that could respond to IL-21. To eliminate contaminating IL-21R$^{+/+}$ T cells from BM, we next used BM from IL-21R KO mice, in combination with SPs from either WT or KO mice. This resulted in enhanced differences in survival between the groups receiving the WT vs IL-21R KO-SP after two months: 0 vs 60% (Figure 1c, $P=0.0001$ by log-rank test), respectively, confirming the former results (Figures 1a and b) and a critical role for IL-21 in GVHD. Consistent with this, clinical GVHD scores in the WT-SP group were higher than those in the IL-21R KO-SP group (Figure 1d).

CD4/CD8 proliferation and serum cytokine levels

To investigate the mechanisms underlying the attenuated GVHD in IL-21R KO-SP transplanted mice, we first counted the number of CD4 and CD8 cells in the spleens 14 days after transplantation. In both IL-21R KO-SP and WT-SP transplanted mice, both cell types were similar in number (Table 1). Next, SPs were stained with carboxyfluorescein diacetate succinimidyl ester to determine their proliferation in mice after transplantation. Both CD4 and CD8 cells from either WT-SP or IL-21R KO-SP transplanted mice showed similar proliferation profiles at day 3 (Figure 2a). Serum concentrations of IFN-γ and IL-4 at day 14 (Figure 2b), those at day 6 (Figure 2c), and IFN-γ and IL-4 produced by recipients' SPs stimulated with allogeneic SPs *in vitro* were comparable between two groups (Figure 2d).

Effects of additional CD4 or CD8 cells on survival

To investigate whether CD4$^+$ T cells are more important for GVHD than CD8$^+$ T cells in our system, we added either WT-CD4$^+$ or IL-21R KO-CD4$^+$ T cells onto the result-predictable transplantation with IL-21R KO-BM and IL-21R KO-SP (Figure 1c). The addition of WT-CD4$^+$ cells resulted in a significantly worse survival than seen with the addition of IL-21R KO-CD4$^+$ cells (Figure 3a, $P=0.0024$, log-rank method). In contrast to this, the difference between WT-CD8$^+$ and IL-21R KO-CD8$^+$ T cells did not reach statistical significance (Figure 3b, $P=0.09$, log-rank method), although they have similar tendency, suggesting that WT-CD4$^+$ rather than WT-CD8$^+$ cells is more important for GVHD, at least in our conditions.

A decoy receptor of IL-21 ameliorates GVHD

To develop a treatment or prophylaxis model in mice and exclude the possibility that the ameliorated GVHD is due to an intrinsic defect in the IL-21R KO-SPs, we designed a decoy receptor of IL-21, which contains its signal sequence, extracellular domain and transmembrane domain, but a truncated intracellular domain. The cDNA encoding this truncated IL-21R was produced by PCR, sequenced, and its extracellular expression in 293 cells was confirmed by flow cytometric analysis using an anti-IL-21R Ab (Figure 4a). In 293 cells, we confirmed that the IL-21R decoy reduced IL-21 concentration in the medium *in vitro* (Figure 4b). Using retroviral transduction, we expressed the decoy receptor in IL-21R KO-BM cells and transplanted them concomitantly with WT-SPs. We carried out three independent experiments and evaluated the survival. Two weeks after transplantation, transduction efficiencies were determined in peripheral blood by measuring green fluorescent protein-positive cells, and were found to be approximately 30–70% (Figure 4c). In an additional experiment, in which transduction efficiency was 40%, the serum concentration of IL-21 was not detectable in decoy receptor transduced BM recipients, whereas those trans-

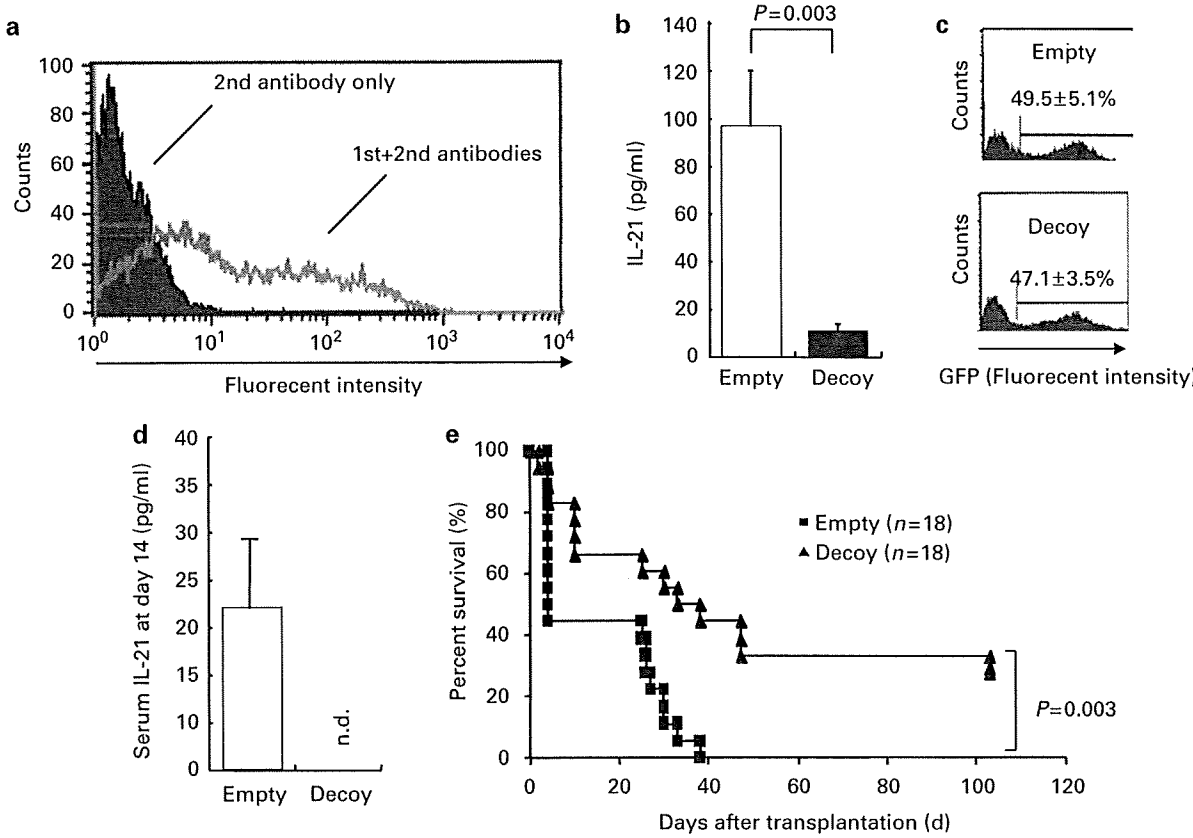

Figure 4 Forced expression of IL-21 decoy receptor ameliorated GVHD. (**a**) Expression of the IL-21 decoy receptor in the 293 cells. (**b**) *In vitro* activity of IL-21 decoy receptor. In all, 293 cells were transduced with either the IL-21 decoy receptor or empty vector, and then recombinant mouse IL-21 (1000 pg/ml) was added to the medium. IL-21 levels were determined by ELISA after 18 h. Shown is mean ± s.d. from three independent experiments ($P=0.003$). (**c**) Transduction efficiency in peripheral blood 2 weeks after transplantation. Transduction efficiency was determined by flow cytometric analysis. Transduced cells are green fluorescent protein (GFP)-positive as the vector contains internal ribosomal entry site (IRES)-GFP. (**d**) Serum concentration of IL-21 at day 14 after transplantation. In this particular experiment, transduction efficiency was approximately 40% in both groups. Total mice analyzed were four empty vector transduced BM recipients and five decoy receptor transduced BM recipients. (**e**) Survival curve after forced expression of the IL-21 decoy receptor. Balb/c recipients were irradiated with 8 Gy and transplanted with wild type splenocytes (5×10^6) and either empty-vector or decoy-receptor transduced BM (starting dose at 5×10^5). Filled squares and filled triangles indicate transplantions with empty-vector transduced BM ($n=18$) and decoy-receptor transduced BM ($n=18$), respectively. The combined results of three independent experiments are shown ($P=0.003$, log-rank test).

duced with the empty vector showed 22 pg/ml on average (Figure 4d), indicating that the decoy receptor significantly diminished serum IL-21 *in vivo*. Although most of the expression was transient, decoy IL-21R-transduced BM resulted in prolonged survival compared with empty-vector transduced BM (Figure 4e, $P=0.003$, log-rank test), suggesting that blockade of the IL-21 signal might be an effective treatment or prophylaxis for GVHD. These results are consistent with the results shown above (Figure 1), and support the hypothesis that IL-21 promotes GVHD.

The attenuated GVHD appeared to be independent of cytotoxic molecules

The significance of cytotoxic molecules such as perforin and granzyme B in GVHD has been reported.[24] To investigate the relationship between these molecules and the attenuated GVHD, we sought to see the levels of expression of these molecules in $CD4^+$ and $CD8^+$ T cells. No clear difference between WT-SP and IL-21R KO-SP transplanted mice was detected (Figure 5a). Moreover, we used a combination of IL-21 decoy receptor and *perforin*-deficient mice. The IL-21 decoy receptor-transduced BM improved survival of recipients with SPs from *perforin*-deficient mice, suggesting that the mechanism of the attenuated GVHD is primarily independent of perforin *in vivo* (Figure 5b). The Fas/FasL system is another cytotoxic molecule and was reported to be important for GVHD rather than GVL.[25,26] To investigate a possible role for Fas/FasL in the attenuated GVHD, we analyzed the effect of IL-21 decoy receptor transduced BM on survival of recipients with SPs from FasL deficient (*gld/gld*) mice and found enhanced survival, suggesting that the mechanism of the attenuated GVHD is also primarily independent of Fas/FasL (Figure 5c).

Discussion

Here, we report that IL-21 is critical for GVHD. SPs from IL-21R$^{-/-}$ (KO) mice induced less severe GVHD than those from WT mice. Moreover, a decoy receptor for IL-21 attenuates GVHD and prolongs survival, confirming the

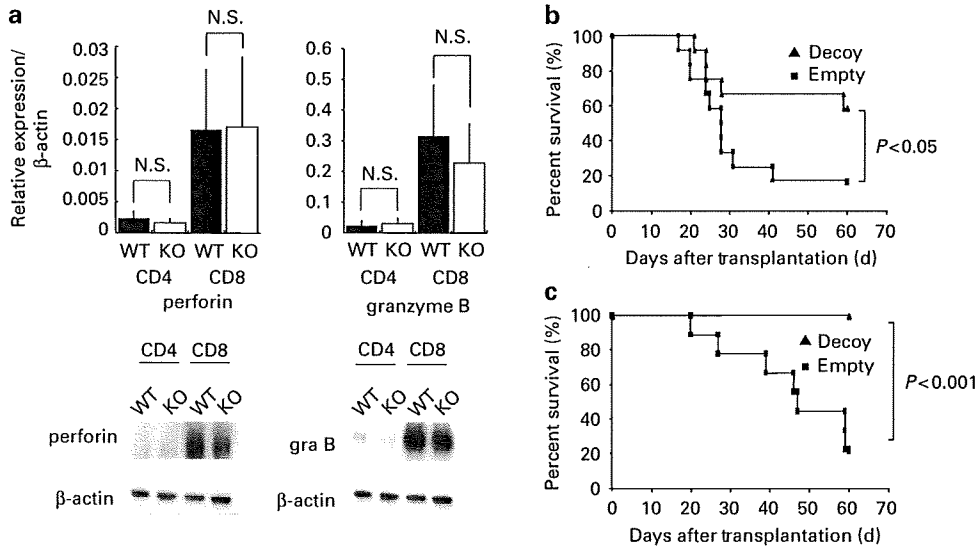

Figure 5 The ameliorated GVHD is dependent on neither FasL nor perforin. (**a**) Perforin and granzyme B expression in CD4/CD8 cells. C57BL/6-DBA2 F1 recipients were transplanted with 1×10^8 splenocytes (SPs) from wild type or IL-21R$^{-/-}$ mice. tRNA and protein were harvested from CD4 or CD8 cells purified from transplanted mice at day 6 after transplantation. Results of RT-qPCR and western blot analysis are shown in upper and lower panel, respectively. (**b**) Survival curve with SPs from perforin deficient mice. C57BL/6-DBA2 F1 recipients were irradiated with 11 Gy and transplanted with either empty-vector or decoy-receptor transduced BM (final cell number: $3–3.2 \times 10^6$) with SPs from perforin-deficient mice ($3.75–5 \times 10^7$). Filled squares and filled triangles indicate transplantations with empty-vector transduced BM ($n = 9$) or decoy-receptor transduced BM ($n = 9$), respectively. The combined results of two independent experiments are shown. *P*-value was calculated by the log-rank method. Transduction efficiencies two weeks after transplantation in peripheral blood were around 30–70% like Figure 4c. (**c**) Survival curve with SPs from FasL deficient mice (*gld/gld* mice). C57BL/6-DBA2 F1 recipients were irradiated with 11 Gy and transplanted with either empty-vector or decoy-receptor transduced BM (final cell number: $3.2–3.5 \times 10^6$) with SPs from *gld/gld* mice ($8–10 \times 10^7$). Filled squares and filled triangles indicate transplantations with empty-vector transduced BM ($n = 12$) or decoy-receptor transduced BM ($n = 12$), respectively. The combined results of two independent experiments are shown. The *P*-value was calculated by the log-rank method.

former experiments with KO mice and suggesting that a possible clinical application of blocking IL-21 for the treatment or prophylaxis of GVHD.

Serum IFN-γ and IL-4 concentrations, CD4/CD8 T-cell proliferation at day 3 after transplantation, and the number of CD4$^+$/CD8$^+$ T cells in spleens of recipients at day 14 after transplantation, all appeared to be comparable between two groups at least under the conditions we have tested. In addition, the decoy IL-21R also ameliorated GVHD induced by *FasL*-deficient and *perforin*-deficient SPs, suggesting that Fas/FasL and perforin are not crucial for the mechanism of the attenuated GVHD by IL-21R KO SPs. However, we could not rule out the possibility that the other transplantation conditions might make the difference more profound and lead to interpretation of the mechanisms. Results of additional CD4$^+$/CD8$^+$ experiments suggested the importance of CD4$^+$ cells. We are now investigating the process by using other transplantation models, such as purified CD4$^+$ T-cell transplantation.

Although we have shown that IL-21 is critical for GVHD in two different systems using both IL-21R KO mice and decoy receptor for IL-21, the molecular mechanisms by which blocking IL-21 attenuates GVHD are not clear at this point.

As the transplantation model we used is an MHC-mismatch CD4$^+$ cell-mediated GVHD, a role for IL-21 in both CD8$^+$ cell-mediated GVHD and MHC-matched GVHD is an area for future investigation.

Here, we opened a new insight for mechanisms of GVHD. These results would help in understanding the mechanisms of GVHD and in developing a treatment for GVHD. In fact, we could demonstrate that IL-21 blockade is a potentially novel approach for the treatment or prophylaxis of GVHD in mouse model. Further *in vivo* and *in vitro* studies, including humans, are required to potentially translate these results from mouse models to human diseases.

Conflict of interest

Drs Katsutoshi Ozaki and Warren J Leonard are inventors on patents and patent applications related to IL-21.

Acknowledgements

We thank Dr Kitamura (Institute of Medical Science, University of Tokyo, Tokyo) for donating PLAT-E, a packaging cell line. This work was supported in part by grants from the Ministry of Health, Labor and Welfare of Japan, by Grants-in-Aid for Scientific Research from the Ministry of Education, Culture, Sports, Science and Technology of Japan, by the Intramural Research Program of the National Heart, Lung and Blood Institute, National Institutes of Health (Bethesda, MD, USA), and by an Intramural Research Grant from Jichi Medical University, Tochigi, Japan.

References

1 Ozaki K, Leonard WJ. Cytokine and cytokine receptor pleiotropy redundancy. *J Biol Chem* 2002; **277**: 29355–29358.

2 Leonard WJ. Cytokines immunodeficiency diseases. *Nat Rev Immunol* 2001; **1**: 200–208.
3 Noguchi M, Yi H, Rosenblatt HM, Filipovich AH, Adelstein S, Modi WS *et al.* Interleukin-2 receptor gamma chain mutation results in X-linked severe combined immunodeficiency in humans. *Cell* 1993; **73**: 147–157.
4 von Freeden-Jeffry U, Vieira P, Lucian LA, McNeil T, Burdach SE, Murray R. Lymphopenia in interleukin (IL)-7 gene-deleted mice identifies IL-7 as a nonredundant cytokine. *J Exp Med* 1995; **181**: 1519–1526.
5 Lodolce JP, Boone DL, Chai S, Swain RE, Dassopoulos T, Trettin S *et al.* IL-15 receptor maintains lymphoid homeostasis by supporting lymphocyte homing and proliferation. *Immunity* 1998; **5**: 669–676.
6 Ozaki K, Spolski R, Feng CG, Qi CF, Cheng J, Sher Au C *et al.* A critical role for IL-21 in regulating immunoglobulin production. *Science* 2002; **298**: 1630–1634.
7 Parrish-Novak J, Dillon SR, Nelson A, Hammond A, Sprecher C, Gross JA *et al.* Interleukin 21 and its receptor are involved in NK cell expansion and regulation of lymphocyte function. *Nature* 2000; **408**: 57–63.
8 Ozaki K, Kikly K, Michalovich D, Young PR, Leonard WJ. Cloning of a type I cytokine receptor most related to the IL-2 receptor beta chain. *Proc Natl Acad Sci USA* 2000; **97**: 11439–114344.
9 Brandt K, Bulfone-Paus S, Foster DC, Ruckert R. Interleukin-21 inhibits dendritic cell activation and maturation. *Blood* 2003; **102**: 4090–4098.
10 Ozaki K, Hishiya A, Hatanaka K, Nakajima H, Wang G, Hwu P *et al.* Overexpression of IL-21 induces expansion of hematopoietic progenitor cells. *Int J Hemat* 2006; **84**: 224–230.
11 Zhou L, Ivanov II, Spolski R, Min R, Shenderov K, Egawa T *et al.* IL-6 programs T(H)-17 cell differentiation by promoting sequential engagement of the IL-21 and IL-23 pathways. *Nat Immunol* 2007; **8**: 967–974.
12 Nurieva R, Yang XO, Martinez G, Zhang Y, Panopoulos AD, Ma L *et al.* Essential autocrine regulation by IL-21 in the generation of inflammatory T cells. *Nature* 2007; **448**: 480–483.
13 Korn T, Bettelli E, Gao W, Awasthi A, Jäger A, Strom TB *et al.* IL-21 initiates an alternative pathway to induce proinflammatory T(H)17 cells. *Nature* 2007; **448**: 484–487.
14 Wurster AL, Rodgers VL, Satoskar AR, Whitters MJ, Young DA, Collins M *et al.* Interleukin 21 is a T helper (Th) cell 2 cytokine that specifically inhibits the differentiation of naive Th cells into interferon gamma-producing Th1 cells. *J Exp Med* 2002; **196**: 969–977.
15 Pesce J, Kaviratne M, Ramalingam TR, Thompson RW, Urban Jr JF, Cheever AW *et al.* The IL-21 receptor augments Th2 effector function and alternative macrophage activation. *J Clin Invest* 2006; **116**: 2044–2055.
16 Fröhlich A, Marsland BJ, Sonderegger I, Kurrer M, Hodge MR, Harris NL *et al.* IL-21 receptor signaling is integral to the development of Th2 effector responses *in vivo*. *Blood* 2007; **109**: 2023–2031.
17 Strengell M, Sareneva T, Foster D, Julkunen I, Matikainen S. IL-21 up-regulates the expression of genes associated with innate immunity and Th1 response. *J Immunol* 2002; **169**: 3600–3605.
18 Ozaki K, Spolski R, Ettinger R, Kim HP, Wang G, Qi CF *et al.* Regulation of B cell differentiation and plasma cell generation by IL-21, a novel inducer of Blimp-1 and Bcl-6. *J Immunol* 2004; **173**: 5361–5371.
19 Bubier JA, Sproule TJ, Foreman O, Spolski R, Shaffer DJ, Morse III HC *et al.* A critical role for IL-21 receptor signaling in the pathogenesis of systemic lupus erythematosus in BXSB-Yaa mice. *Proc Natl Acad Sci USA* 2009; **106**: 1518–1523.
20 Spolski R, Kashyap M, Robinson C, Yu Z, Leonard WJ. IL-21 signaling is critical for the development of type I diabetes in the NOD mouse. *Proc Natl Acad Sci USA* 2008; **105**: 14028–14033.
21 Sutherland AP, Van Belle T, Wurster AL, Suto A, Michaud M, Zhang D *et al.* IL-21 is required for the development of type 1 diabetes in NOD mice. *Diabetes* 2009; **58**: 1144–1155.
22 Shlomchik WD. Graft-versus-host disease. *Nat Rev Immunol* 2007; **7**: 340–352.
23 Cooke KR, Kobzik L, Martin TR, Brewer J, Delmonte Jr J, Crawford JM *et al.* An experimental model of idiopathic pneumonia syndrome after bone marrow transplantation: I. The roles of minor H antigens and endotoxin. *Blood* 1996; **88**: 3230–3239.
24 Graubert TA, DiPersio JF, Russell JH, Ley TJ. Perforin/granzyme-dependent and independent mechanisms are both important for the development of graft-versus-host disease after murine bone marrow transplantation. *J Clin Invest* 1997; **100**: 904–911.
25 Tsukada N, Kobata T, Aizawa Y, Yagita H, Okumura K. Graft-versus-leukemia effect and graft-versus-host disease can be differentiated by cytotoxic mechanisms in a murine model of allogeneic bone marrow transplantation. *Blood* 1999; **93**: 2738–2747.
26 Schmaltz C, Alpdogan O, Horndasch KJ, Muriglan SJ, Kappel BJ, Teshima T *et al.* Differential use of Fas ligand and perforin cytotoxic pathways by donor T cells in graft-versus-host disease and graft-versus-leukemia effect. *Blood* 2001; **97**: 2886–2895.

ELSEVIER

Experimental Hematology

Experimental Hematology 2009;37:1250–1257

Cotransplantation with MSCs improves engraftment of HSCs after autologous intra-bone marrow transplantation in nonhuman primates

Shigeo Masuda[a], Naohide Ageyama[b], Hiroaki Shibata[b], Yoko Obara[c], Tamako Ikeda[a], Kengo Takeuchi[d], Yasuji Ueda[e], Keiya Ozawa[c], and Yutaka Hanazono[a]

[a]*Division of Regenerative Medicine, Center for Molecular Medicine, Jichi Medical University, Tochigi, Japan;* [b]*Tsukuba Primate Research Center, National Institute of Biomedical Innovation, Ibaraki, Japan;* [c]*Division of Hematology, Department of Medicine, Jichi Medical University, Tochigi, Japan;* [d]*Division of Pathology, The Cancer Institute, Tokyo, Japan;* [e]*Department of Gene Therapy, Graduate School of Medicine, Chiba University, Chiba, Japan*

(Received 18 June 2009; revised 21 July 2009; accepted 22 July 2009)

Objective. **Hematopoietic stem cells (HSCs) reside in the osteoblastic niche, which consists of osteoblasts. Mesenchymal stromal cells (MSCs) have an ability to differentiate into osteoblasts. Here, using nonhuman primates, we investigated the effects of cotransplantation with MSCs on the engraftment of HSCs after autologous intra-bone marrow transplantation.**

Materials and Methods. **From three cynomolgus monkeys, CD34-positive cells (as HSCs) and MSCs were obtained. The former were divided into two equal aliquots and each aliquot was genetically marked with a distinctive retroviral vector to track the in vivo fate. Each HSC aliquot with or without MSCs was autologously injected into the bone marrow (BM) cavity of right or left side, enabling the comparison of in vivo fates of the two HSC grafts in the same body.**

Results. **In the three monkeys, $CD34^+$ cells transplanted with MSCs engrafted 4.4, 6.0, and 1.6 times more efficiently than $CD34^+$ cells alone, as assessed by BM colony polymerase chain reaction. In addition, virtually all marked cells detected in the peripheral blood were derived from the cotransplantation aliquots. Notably, colony-forming units derived from the cotransplantation aliquots were frequently detected in BM distant sites from the injection site, implying that cotransplantation with MSCs also restored the ability of gene-marked HSCs to migrate and achieve homing in the distant BM.**

Conclusion. **Cotransplantation with MSCs would improve the efficacy of transplantation of gene-modified HSCs in primates, with enhanced engraftment in BM as well as increased chimerism in peripheral blood through migration and homing.** © **2009 ISEH - Society for Hematology and Stem Cells. Published by Elsevier Inc.**

Hematopoietic stem cells (HSCs) have been shown to reside in the hematopoietic niche, such as the osteoblastic or vascular niche [1,2]. The osteoblastic niche is provided by bone marrow (BM) osteoblasts, which are derived from mesenchymal stromal cells (MSCs) [3–5]. Although conditioning, such as total body irradiation or administration of busulfan, would be required for successful engraftment of transplanted HSCs, the treatment may destroy the osteoblastic niche, hampering engraftment [6]. If an osteoblastic niche could be generated through cotransplantation with MSCs, the engraftment of HSCs would be enhanced; however, MSCs cannot home to or engraft in BM when transplanted via vessels [7]. On the other hand, the direct transplantation of HSCs into a BM cavity, namely intra-bone marrow transplantation (iBMT), improves engraftment of HSCs compared with intravascular transplantation [8–13]. In fact, one clinical trial of iBMT has been published recently [14] that demonstrates early donor engraftment

Offprint requests to: Yutaka Hanazono, M.D., Ph.D., Division of Regenerative Medicine, Center for Molecular Medicine, Jichi Medical University, 3311-1 Yakushiji, Shimotsuke-shi, Tochigi 329-0498, Japan; E-mail: hanazono@jichi.ac.jp

Supplementary data associated with this article can be found, in the online version, at doi:10.1016/j.exphem.2009.07.008.

0301-472X/09 $–see front matter.
doi: 10.1016/j.exphem.2009.07.008

after allogeneic iBMT, suggesting safety and efficacy of iBMT. Previous studies have demonstrated that cotransplantation with MSCs improves engraftment of HSCs in mice [15–17], especially after iBMT [18]. However, neither systematic human nor large animal's studies have been conducted to evaluate the efficacy of cotransplantation with MSCs.

To assess the efficacy of cotransplantation with MSCs in nonhuman primates, we applied hemi-iBMT in cynomolgus monkeys; i.e., the BM on one side (right or left) of the body was transplanted with HSCs together with MSCs and the other side was transplanted with HSCs alone. We genetically marked HSCs before transplantation with two distinct retroviral vectors to identify transplanted cells derived from the two HSC aliquots and to compare their in vivo fates [19,20]. This hemi-iBMT method combined with the dual genetic marking technique enables us to evaluate the results in the same body, comparing the outcomes of cells of interest with that of control cells; thus, there is no need to consider the variation in results among monkeys. Here we show that cotransplantation with MSCs improves engraftment of HSCs after iBMT in nonhuman primates.

Materials and methods

Animals

Cynomolgus macaques (*Macaca fascicularis*) were housed and handled in accordance with the Rules for Care and Management at the Tsukuba Primate Research Center (Ibaraki, Japan) and with the Guiding Principles for Animal Experiments using Non-Human Primates formulated by the Primate Society of Japan. The protocol of the experimental procedures was approved by the Animal Welfare and Animal Care Committee of the National Institute of Biomedical Innovation (Osaka, Japan).

Isolation of cynomolgus MSCs and CD34$^+$ cells

BM cells were collected by aspiration from the iliac bone of cynomolgus monkeys and processed as described previously [13,21]. From the harvested cells, the nucleated cell fraction was obtained after red blood cell lysis with ACK buffer (155 mM NH_4Cl, 10 mM $KHCO_3$, and 0.1 mM ethylenediamine tetraacetic acid; Wako, Osaka, Japan). MSCs were isolated by plastic adherence for 1 hour, and cultured for 2 to 3 weeks (i.e., three to four passages) in Dulbecco's modified Eagle's medium supplemented with 20% fetal bovine serum and penicillin/streptomycin at 37°C with 5% CO_2. After isolation of adherent cells, nonadherent cells were enriched for CD34$^+$ cells by magnet beads conjugated with anti-human CD34 (clone 561; Dynal, Lake Success, NY, USA) which cross-reacts with cynomolgus CD34 [21]. The purity of CD34$^+$ cells ranged from 90% to 95%, as assessed with another anti-human CD34 (clone 563; Pharmingen, San Diego, CA, USA) which cross-reacts with cynomolgus CD34 [21]. Mean enrichment after the selection of CD34$^+$ cells was 84-fold in terms of colony-forming units (CFUs).

Retroviral transduction

We used G1Na and LNL6 retroviral vectors expressing the neomycin resistance gene (*neo^R*) [19,20]. Titers of the viral supernatants used in the present study were both 1×10^6 particles/μL, as assessed by Retrovirus Titer Set (for real-time polymerase chain reaction [PCR]) according to manufacturer's instruction (Takara, Shiga, Japan). CD34$^+$ cells were cultured at starting concentrations of 1 to 5×10^5 cells/mL in vector supernatant (frozen-and-thawed once) of G1Na or LNL6. Four-day transduction (one supernatant transduction per day) with recombinant human stem cell factor (SCF), recombinant human Fms-like tyrosine kinase 3 ligand (Flt3-ligand) (R&D Systems, Minneapolis, MI, USA), and recombinant human thrombopoietin (Kirin, Tokyo, Japan) each at 100 ng/mL in dishes coated with 20 μg/cm^2 of RetroNectin (Takara, Shiga, Japan) was conducted as described previously [13]. After 4-day transduction, cells were washed, frozen, and stocked until transplantation.

iBMT

Before transplantation, conditioning was performed; either total body irradiation (550 cGy×2) in the first monkey examined, or administration of busulfan (Busulfex) in the second (8 mg/kg×2) and third (10 mg/kg×1) monkey. After conditioning, monkeys were anesthetized and two needles were inserted into both ends of the femur or humerus [13,22]. A syringe containing 50 mL heparin-added saline was connected to one needle and an empty syringe was connected to the other. Normal saline was irrigated gently from one syringe to another through the marrow cavity twice to remove BM cells physically. Then, gene-marked CD34$^+$ cells with or without MSCs were suspended in 500 μL phosphate-buffered saline (PBS) containing 50% autologous serum, and injected into the marrow cavity.

Sampling of BM cells and peripheral blood cells

One or two months after transplantation, peripheral blood (PB) and BM cells were taken to assess the in vivo fate of two aliquots. PB cells were collected routinely post-transplantation. To harvest BM cells, monkeys were sacrificed, the ilium marrow was aspirated using BM needles, and the limb marrow was taken by irrigation with PBS.

Clonogenic hematopoietic progenitor assays

Cells were plated in a 35-mm Petri dish in 1 mL MethoCult GF$^+$ H4435 (StemCell Technologies, Vancouver, BC, Canada). After incubation for 14 days at 37°C with 5% CO_2, colonies containing >50 cells were counted using an inverted light microscope, and plucked for PCR as described here. Experiments were conducted in triplicate.

PCR

All the procedures were followed in detail as described previously [13]. From PB nucleated cells, genomic DNA was extracted using the QIAamp DNA Blood Mini Kit (Qiagen, Chatsworth, CA, USA). From BM colonies, genomic DNA was extracted as follows; well-separated, individual colonies at day 14 were plucked into 50 μL distilled water, and digested with 20 μg/mL proteinase K (Takara, Shiga, Japan) at 56°C overnight, followed by 99°C for 10 minutes. For the semi-quantitative PCR of PB samples, DNA (50 ng) was amplified in triplicate with *neo^R*-specific primers for both G1Na and LNL6 (5′-TCCAT CATGGCTGATGCAATGCGGC-3′ and 5′-GATAGAAGGCGAT-GCGCTGCGAATCG-3′). The final sizes of the PCR products were 435 base pairs (bp) for both G1Na and LNL6. For PCR of BM colonies, the outer primer set for both G1Na and LNL6 vector was 5′-GGCCAGACTGTTACCACTCC-3′ and 5′-CAGT CATAGCCGAATAGCCTCT-3′, and the inner primer set for

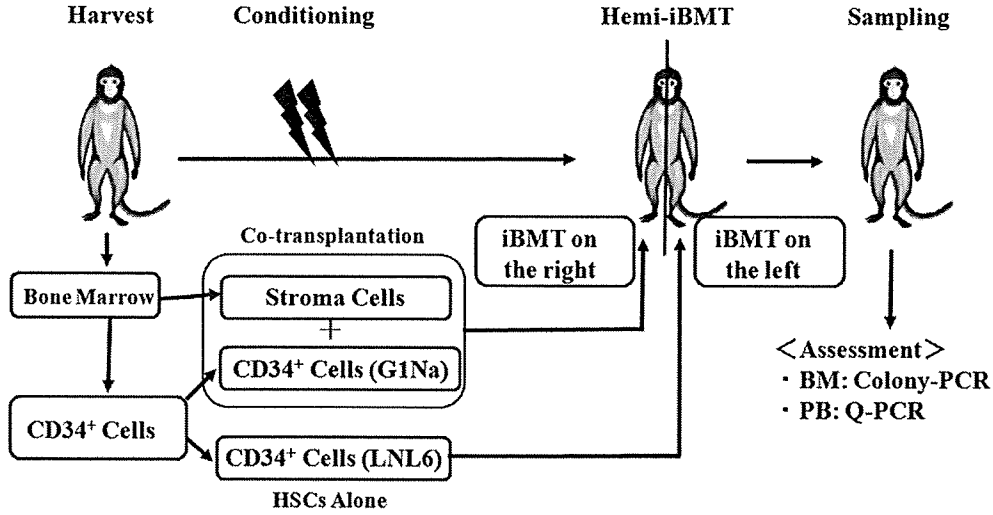

Figure 1. Study design using cynomolgus monkeys. Autologous bone marrow (BM) cells were harvested and separated into two populations, either adherent stromal cells or nonadherent cells. From the nonadherent cells, $CD34^+$ cells were purified (referred to as hematopoietic stem cells [HSCs]), and divided into two equal aliquots. Each aliquot was genetically marked with a distinctive neo^R-retroviral vector, G1Na or LNL6. The stromal cells (referred to as mesenchymal stromal cells [MSCs]) were expanded ex vivo, and then transplanted together with HSCs as a cotransplantation aliquot into the right side of the BM cavity after conditioning. The other aliquot of HSCs was transplanted alone into the left side of the BM cavity of the same body, namely hemi intra-bone marrow transplantation (iBMT). After transplantation, BM and peripheral blood (PB) cells were taken and subjected to colony and semi-quantitative polymerase chain reaction (Q-PCR), respectively.

both G1Na and LNL6 vector was 5′-CGGATCGCTCACAAC CAGTC-3′ and 5′-AGAACCTGCGTGCAATCCATC-3′. The final sizes of the nested PCR products were 455 and 439 bp for G1Na and LNL6, respectively. The final PCR products were separated on 2% agarose gels, or analyzed by capillary electrophoresis (HAD-GT12 System; Qiagen), which allows distinguishing of the sizes of DNA products (16-bp difference) in high resolution.

Statistics

Statistical analyses were performed using Student's *t*-test. A p value <0.05 was considered statistically significant.

Results

Improved engraftment of HSCs after cotransplantation with MSCs

We examined whether gene-marked $CD34^+$ cells with MSCs would engraft more efficiently than those without MSCs after iBMT in a cynomolgus autologous transplantation model. We performed hemitransplantation (Fig. 1); the concept has been explained in the introduction. $CD34^+$ cells were isolated from three monkeys and divided into two equal aliquots. Each aliquot was transduced with the neo^R-expressing retroviral vector G1Na or LNL6. The mean transduction efficiency was 74.0% with no marked differences between the two vectors (Table 1). We injected the transduced $CD34^+$ cells with or without MSCs directly into the BM cavity after gently irrigating the cavity with saline. The procedure was safely conducted without pulmonary embolism or infection of BM. After iBMT, we compared the engraftment of the two aliquots by BM colony PCR; that is, we plated BM cells in methylcellulose medium and examined resulting colonies for the provirus by PCR. Schematic representation of the study design is shown in Figure 1.

Table 1. Ex vivo transduction and transplantation

Animal (ID no.)	Sex/Age (y)/ body weight (kg)	Groups of hemi-iBMT	Vectors for marking	No. of infused $CD34^+$ cells/kg	Fraction of provirus-positive CFUs in infused $CD34^+$ cells (%)	No. of infused MSCs/kg
Monkey 1 (H025)	Male/5/3.5	Cotransplant*	G1Na	4.1×10^6	7/12 (58.3)	3.0×10^6
		HSC alone	LNL6	3.3×10^6	6/11 (54.5)	0
Monkey 2 (H030)	Male/8/6.5	Cotransplant*	LNL6	3.4×10^5	23/33 (69.7)	7.7×10^5
		HSC alone	G1Na	2.8×10^5	27/30 (90.0)	0
Monkey 3 (H033)	Male/8/6.2	Cotransplant*	G1Na	6.6×10^4	11/13 (78.6)	5.2×10^5
		HSC alone	LNL6	7.1×10^4	13/14 (92.9)	0

CFUs=colony-forming units; HSC=hematopoietic stem cell; iBMT=intra-bone marrow transplantation; MSCs=mesenchymal stromal cells.
*Cotransplant means transplantation of HSCs combined with MSCs.

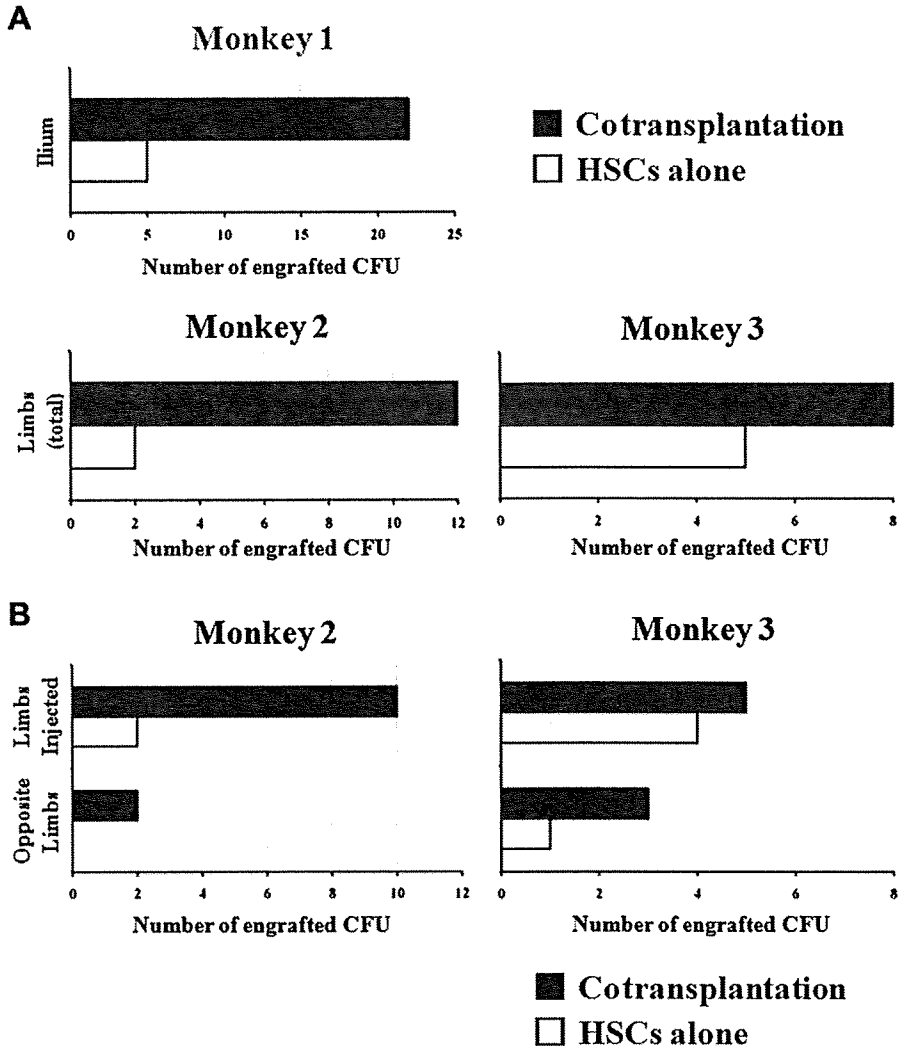

Figure 2. Improved engraftment of hematopoietic stem cells (HSCs) after cotransplantation with mesenchymal stromal cells (MSCs). (**A**) Efficacy of cotransplantation with MSCs. The numbers of engrafted gene-marked colony-forming units (CFUs) are shown, either derived from the cotransplantation aliquots (black columns) or from the HSC-alone aliquots (white columns). After sacrificing the animals, BM cells were harvested from the ilium in Monkey 1 and from the limbs (humerus and femur of both sides) in Monkeys 2 and 3. Total numbers of CFUs marked with G1Na or LNL6 from the marrow samples of each animal are indicated. (**B**) The engraftment site of gene-marked CFUs. Numbers of gene-marked CFUs detected in the limbs of either the injection or opposite side are separately shown for each aliquot.

In the first monkey examined (Monkey 1), one HSC aliquot, genetically marked with G1Na, was transplanted into the right side together with MSCs, while another HSC aliquot, genetically marked with LNL6, was transplanted into the left side without MSCs. At day 46 after transplantation, the cotransplantation aliquot engrafted 4.4 times more efficiently than the HSC-alone aliquot, as assessed by colony PCR of the ilium marrow that was neutral from both sides (47.8% vs 10.9%, respectively) (Table 2 and Fig. 2A). In the second monkey (Monkey 2), hemi-iBMT was conducted with the switching of vectors to exclude the possibility of a vector-associated bias. The cotransplantation aliquot again engrafted more efficiently (6.0 times) than the HSC-alone aliquot, as assessed by colony PCR of marrow from the four limbs at day 39 after transplantation (6.0% vs 1.0%, respectively) (Table 2 and Fig. 2A). In the third monkey (Monkey 3), the cotransplantation aliquot engrafted more efficiently than the HSC-alone aliquot at day 56 after transplantation, although the difference in this monkey was not as significant, as assessed by colony PCR (7.1% vs 4.5%, respectively) (Table 2 and Fig. 2A). These results suggest that cotransplantation with MSCs improves engraftment of HSCs in nonhuman primates.

In addition, in two of the three animals (Monkeys 2 and 3), CFUs derived from the cotransplantation aliquots were detected in the BM of the opposite side (Fig. 2B), implying that the transduced $CD34^+$ cells injected into the BM might migrate and achieve homing to the distant BM.

Table 2. In vivo transduction levels post-transplantation with or without MSCs

Animal (ID no.)	Groups of hemi-iBMT	Site of iBMT	Vectors for marking	Sampling of BM* (post-transplantation)	In vivo marking (% of provirus-positive colonies)	Fold increase in engrafted CFUs†
Monkey 1 (H025)	Cotransplant	Right humerus/femur	G1Na	Ilium (day 46)	22/46 (47.8)	4.4
	HSC alone	Left humerus/femur	LNL6		5/46 (10.9)	
Monkey 2 (H030)	Cotransplant	Right humerus/femur	LNL6	Limbs (day 39)	12/192 (6.0)	6.0
	HSC alone	Left humerus/femur	G1Na		2/192 (1.0)	
Monkey 3 (H033)	Cotransplant	Right humerus/femur	G1Na	Limbs (day 56)	8/112 (7.1)	1.6
	HSC alone	Left humerus/femur	LNL6		5/112 (4.5)	

BM=bone marrow; iBMT=intra-bone marrow transplantation; MSCs=mesenchymal stromal cells.
*Bone marrow cells were taken from the ilium and/or limbs (humerus and femur on both sides).
†Fold increase in engrafted colony-forming units (CFUs) was calculated by dividing the number of CFUs derived from cotransplantation aliquots by that from hematopoietic stem cell (HSC)-alone aliquots.

Origin of marked cells in PB

Although there were no marked cells detected in the PB in Monkey 1, 2.0% and 0.4% of the PB cells were marked in Monkeys 2 and 3 on days 33 and 35 post-transplantation, respectively, as assessed by semiquantitative PCR (Fig. 3A). With capillary electrophoresis, which can detect a 16-bp difference between G1Na and LNL6, these cells were proven to be marked with the vector for the cotransplant aliquot (Fig. 3B). In all monkeys examined, cells derived from the HSC-alone aliquots were barely detected in the PB. These results clearly indicate that cotransplantation with MSCs enhances transplant-derived chimerism in the PB.

Mechanism of improvements by MSCs

Previous studies demonstrated that, in human-mouse xenograft models, transplanted human MSCs, after their differentiation into osteoblasts, osteocytes, and endothelial cells, appeared to be involved in the maintenance of human hematopoiesis through two ways: via their physical interaction with primitive hematopoietic cells [18] and via factors they secrete, such as stromal derived factor-1 (SDF-1) [18], which have been shown to regulate the proliferation and survival of hematopoietic stem and progenitor cells [12,23–25]. To assess the former possibility, we retrovirally marked MSCs with the β-galactosidase gene before transplantation in Monkey 3, but could not detect LacZ-positive cells in the BM (data not shown), possibly due to the low expression level or immune clearance of LacZ. As grounds of the latter possibility, it has been reported that the expression of hematopoiesis-supporting cytokines including SCF, SDF-1, and angiopoietin-1 was upregulated in preadipocytes during differentiation from MSCs [26]. Contrary to our expectations, we found the reverse tendency: decreased concentrations of these cytokines in the BM transplanted with HSCs and MSCs as compared to those with HSCs alone, albeit not at significant levels (SDF-1α, $p=0.21$; SCF, $p=0.46$; angiopoietin-1; $p=0.39$; Supplementary Figure E1 (online only, available at www.exphem.org). It is possible to speculate that poor engraftment with HSCs alone might stimulate compensatory signaling pathways to upregulate the expression of these hematopoiesis-supporting cytokines.

Discussion

Clinical trials to intravenously coinfuse MSCs have already been reported both in the autologous [27] and allogeneic [28,29] settings; however, they aimed at feasibility and safety, and are not controlled studies. We obtained the favorable results in terms of engraftment of HSCs in the controlled autologous setting in monkeys.

Although the migration of HSCs post-transplantation has already been demonstrated in mouse syngeneic iBMT, human-mouse xeno-iBMT, and monkey auto-iBMT models [8,10–13], it has been reported that ex vivo cultured HSCs lose their capacity for migration and homing [30]. However, there was still a residual capacity for migration in ex vivo manipulated HSCs without cotransplantation of MSCs in our study (Fig. 2B). After cotransplantation with MSCs, the ex vivo manipulated HSCs began to migrate to the distant BM much more frequently, suggesting that cotransplanted MSCs restored the properties of HSCs for migration and homing, at least in part. Moreover, the efficacy of MSCs was much more marked in the PB rather than in the BM, implying that MSCs might have some effects on the mobilization steps.

Our setting of hemitransplantation with dual genetic marking allows tracking and comparison of two HSC grafts with or without MSCs in the same monkeys, and thus it is meritorious for evaluation of migration and homing as described here. It is also useful, considering that there are large individual differences in outbred monkeys, unlike mice. Individual differences in monkeys often overwhelm differences in experimental data. In fact, the differences in the engraftment post-transplantation among Monkeys 1 to 3 (up to 10-fold) are apparently larger than the differences in the engraftment between the two HSC grafts (up to 6.0-fold) (Table 2).

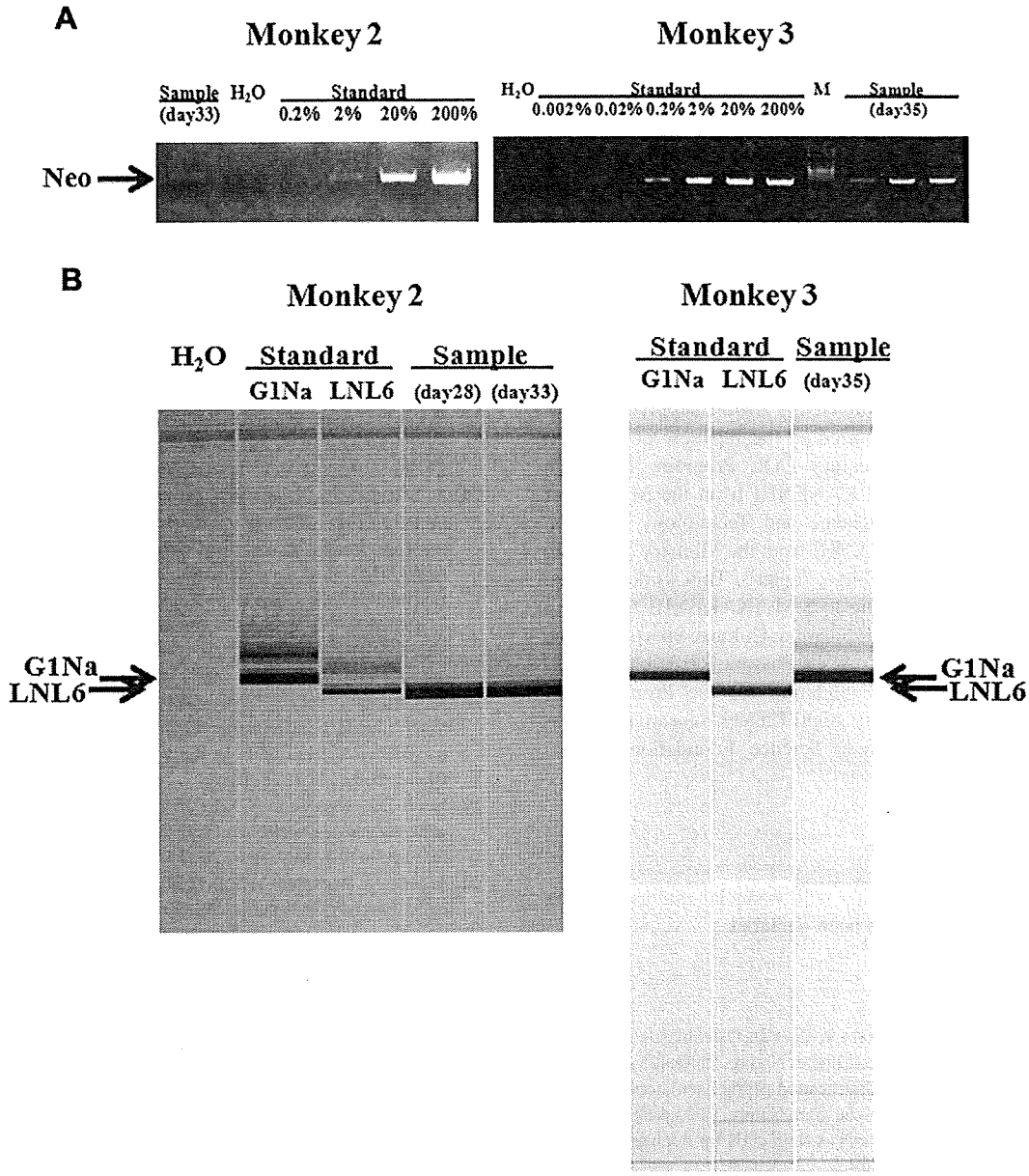

Figure 3. Contribution of transplant-derived cells to the peripheral blood (PB). (**A**) Polymerase chain reaction (PCR) products separated on agarose gels. The genomic DNA extracted from the PB of Monkey 2 on day 33 and Monkey 3 on day 35 post-transplantation was subjected to semiquantitative PCR for the vector neo^R sequence. Neo^R-marked cells were detected in the PB after transplantation. Positive controls corresponding to 0.002%, 0.02%, 0.2%, 2%, 20%, and 200% of marked cells were included. (**B**) Capillary electrophoresis of PCR products. The PCR products in (**A**) were subjected to capillary electrophoresis with positive controls. This technique enables us to distinguish G1Na and LNL6 markings with only a 16-bp difference. Upper and lower bands denote G1Na and LNL6, respectively. The detected bands in the PB were all derived from the cotransplantation aliquots.

Current literature on the subject of coinfusion of MSCs with HSCs in an allogeneic setting suggests that enhanced engraftment is achieved via dampening of the immune response against donor HSCs [28,29]. Such a mechanism cannot be formally ruled out, even in our autologous setting, because transplanted HSCs were genetically modified to express a foreign gene (neo^R).

Although the efficacy of cotransplantation with MSCs was suggested, the overall rate of HSCs engraftment in this study appears to be low, as is the case in other studies using nonhuman primates [31,32]. Further improvements should be needed to apply these methods to human trials. We did not follow the animals long-term in the present study. We would like to see whether or not cotransplantation with MSCs brings better engraftment. Thus, we euthanized monkeys at 1 to 2 months post-transplantation to harvest all the ilium and limbs marrow and we could not follow them longer-term. Therefore, the present results will reflect the behavior of short-term hematopoietic repopulating cells, and longer follow-up (at least 180 day) should be needed to

evaluate the long-term efficacy of cotransplantation with MSCs. There also remains a concern over safety. Because we used ex vivo expanded MSCs, there is a possibility of causing tumors, such as osteosarcoma. Longer-term studies are needed to assess safety as well.

Acknowledgments

We thank Y. Katakai (The Corporation for Production and Research of Laboratory Primates [Ibaraki, Japan]) for animal care and Y. Furukawa (Jichi Medical University [Tochigi, Japan]) for technical help. G1Na and LNL6 were kindly provided by C. E. Dunbar (Hematology Branch, National Heart, Lung, and Blood Institute [Bethesda, MD, USA], National Institutes of Health [Bethesda, MD, USA]). We acknowledge Kirin's supply of thrombopoietin. This study was supported by the Japanese government grants to Y.H. (JMS 21st Century COE Program, High-tech Research Center Program, and KAKENHI from the Ministry of Education, Culture, Sports, Science and Technology of Japan [Tokyo, Japan], as well as KAKENHI from the Ministry of Health, Labor and Welfare of Japan [Tokyo, Japan]). This work was also in part supported by the funding to S.M. (KAKENHI for Young Scientists from the Ministry of Education, Culture, Sports, Science and Technology of Japan, Mitsubishi Pharma Research Foundation [Osaka, Japan], Kanae Foundation for the Promotion of Medical Science [Tokyo, Japan], Aichi Cancer Research Foundation [Aichi, Japan], and Takeda Science Foundation [Osaka, Japan]).

Conflict of Interest

No financial interest/relationships with financial interest relating to the topic of this article have been declared.

References

1. Calvi LM, Adams GB, Weibrecht KW, et al. Osteoblastic cells regulate the haematopoietic stem cell niche. Nature. 2003;425:841–846.
2. Zhang J, Niu C, Ye L, et al. Identification of the haematopoietic stem cell niche and control of the niche size. Nature. 2003;425:836–841.
3. Prockop DJ. Marrow stromal cells as stem cells for nonhematopoietic tissues. Science. 1997;276:71–74.
4. Pittenger MF, Mackay AM, Beck SC, et al. Multilineage potential of adult human mesenchymal stem cells. Science. 1999;284:143–147.
5. Ozawa K, Sato K, Oh I, et al. Cell and gene therapy using mesenchymal stem cells (MSCs). J Autoimmun. 2008;30:121–127.
6. Plett PA, Frankovitz SM, Orschell-Traycoff CM. In vivo trafficking, cell cycle activity, and engraftment potential of phenotypically defined primitive hematopoietic cells after transplantation into irradiated or nonirradiated recipients. Blood. 2002;100:3545–3552.
7. Wynn RF, Hart CA, Corradi-Perini C, et al. A small proportion of mesenchymal stem cells strongly expresses functionally active CXCR4 receptor capable of promoting migration to bone marrow. Blood. 2004;104:2643–2645.
8. Zhong JF, Zhan Y, Anderson WF, et al. Murine hematopoietic stem cell distribution and proliferation in ablated and nonablated bone marrow transplantation. Blood. 2002;100:3521–3526.
9. Nakamura K, Inaba M, Sugiura K, et al. Enhancement of allogeneic hematopoietic stem cell engraftment and prevention of GVHD by intra-bone marrow transplantation plus donor lymphocyte infusion. Stem Cells. 2004;22:125–134.
10. Wang J, Kimura T, Asada R, et al. SCID-repopulating cell activity of human cord blood-derived CD34- cells assured by intra-bone marrow injection. Blood. 2003;101:2924–2931.
11. Mazurier F, Doedens M, Gan OI, et al. Rapid myeloerythroid repopulation after intrafemoral transplantation of NOD-SCID mice reveals a new class of human stem cells. Nat Med. 2003;9:959–963.
12. Yahata T, Ando K, Sato T, et al. A highly sensitive strategy for SCID-repopulating cell assay by direct injection of primitive human hematopoietic cells into NOD/SCID mice bone marrow. Blood. 2003;101:2905–2913.
13. Ueda K, Hanazono Y, Shibata H, et al. High-level in vivo gene marking after gene-modified autologous hematopoietic stem cell transplantation without marrow conditioning in nonhuman primates. Mol Ther. 2004;10:469–477.
14. Frassoni F, Gualandi F, Podestà M, et al. Direct intrabone transplant of unrelated cord-blood cells in acute leukaemia: a phase I/II study. Lancet Oncol. 2008;9:831–839.
15. Noort WA, Kruisselbrink AB, in 't Anker PS, et al. Mesenchymal stem cells promote engraftment of human umbilical cord blood-derived CD34(+) cells in NOD/SCID mice. Exp Hematol. 2002;30:870–878.
16. in 't Anker PS, Noort WA, Kruisselbrink AB, et al. Nonexpanded primary lung and bone marrowderived mesenchymal cells promote the engraftment of umbilical cord blood-derived CD34(+) cells in NOD/SCID mice. Exp Hematol. 2003;31:881–889.
17. Bensidhoum M, Chapel A, Francois S, et al. Homing of in vitro expanded Stro-1^- or Stro-1^+ human mesenchymal stem cells into the NOD/SCID mouse and their role in supporting human CD34 cell engraftment. Blood. 2004;103:3313–3319.
18. Muguruma Y, Yahata T, Miyatake H, et al. Reconstitution of the functional human hematopoietic microenvironment derived from human mesenchymal stem cells in the murine bone marrow compartment. Blood. 2006;107:1878–1887.
19. Heim DA, Hanazono Y, Giri N, et al. Introduction of a xenogeneic gene via hematopoietic stem cells leads to specific tolerance in a rhesus monkey model. Mol Ther. 2000;1:533–544.
20. Tisdale JF, Hanazono Y, Sellers SE, et al. Ex vivo expansion of genetically marked rhesus peripheral blood progenitor cells results in diminished long-term repopulating ability. Blood. 1998;92:1131–1141.
21. Shibata H, Hanazono Y, Ageyama N, et al. Collection and analysis of hematopoietic progenitor cells from cynomolgus macaques (Macaca fascicularis): assessment of cross-reacting monoclonal antibodies. Am J Primatol. 2003;61:3–12.
22. Kushida T, Inaba M, Ikebukuro K, et al. Comparison of bone marrow cells harvested from various bones of cynomolgus monkeys at various ages by perfusion or aspiration methods: a preclinical study for human BMT. Stem Cells. 2002;20:155–162.
23. Lataillade JJ, Clay D, Dupuy C, et al. Chemokine SDF-1 enhances circulating CD34(+) cell proliferation in synergy with cytokines: possible role in progenitor survival. Blood. 2000;95:756–768.
24. Lataillade JJ, Clay D, Bourin P, et al. Stromal cell derived factor 1 regulates primitive hematopoiesis by suppressing apoptosis and by promoting G(0)/G(1) transition in CD34(+) cells: evidence for an autocrine/paracrine mechanism. Blood. 2002;99:1117–1129.
25. Cashman J, Clark-Lewis I, Eaves A, Eaves C. Stromal-derived factor 1 inhibits the cycling of very primitive human hematopoietic cells in vitro and in NOD/SCID mice. Blood. 2002;99:792–799.
26. Oh I, Ozaki M, Miyazato A, et al. Screening of genes responsible for differentiation of mouse mesenchymal stromal cells by DNA microarray analysis of C3H10T1/2 and C3H10T1/2-derived cell lines. Cytotherapy. 2007;9:80–90.
27. Koç ON, Gerson SL, Cooper BW, et al. Rapid hematopoietic recovery after coinfusion of autologous-blood stem cells and culture-expanded marrow mesenchymal stem cells in advanced breast cancer patients receiving high-dose chemotherapy. J Clin Oncol. 2000;18:307–316.
28. Lazarus HM, Koc ON, Devine SM, et al. Cotransplantation of HLA-identical sibling culture-expanded mesenchymal stem cells and

hematopoietic stem cells in hematologic malignancy patients. Biol Blood Marrow Transplant. 2005;11:389–398.
29. Ball LM, Bernardo ME, Roelofs H, et al. Cotransplantation of ex vivo expanded mesenchymal stem cells accelerates lymphocyte recovery and may reduce the risk of graft failure in haploidentical hematopoietic stem-cell transplantation. Blood. 2007;110:2764–2767.
30. Yamamura K, Ohishi K, Masuya M, et al. Ex vivo culture of human cord blood hematopoietic stem/progenitor cells adversely influences their distribution to other bone marrow compartments after intrabone marrow transplantation. Stem Cells. 2008;26:543–549.
31. Larochelle A, Choi U, Shou Y, et al. In vivo selection of hematopoietic progenitor cells and temozolomide dose intensification in rhesus macaques through lentiviral transduction with a drug resistance gene. J Clin Invest. 2009;119:1952–1963.
32. Zhang XB, Beard BC, Beebe K, Storer B, Humphries RK, Kiem HP. Differential effects of HOXB4 on nonhuman primate short- and long-term repopulating cells. PLoS Med. 2006;3:e173.

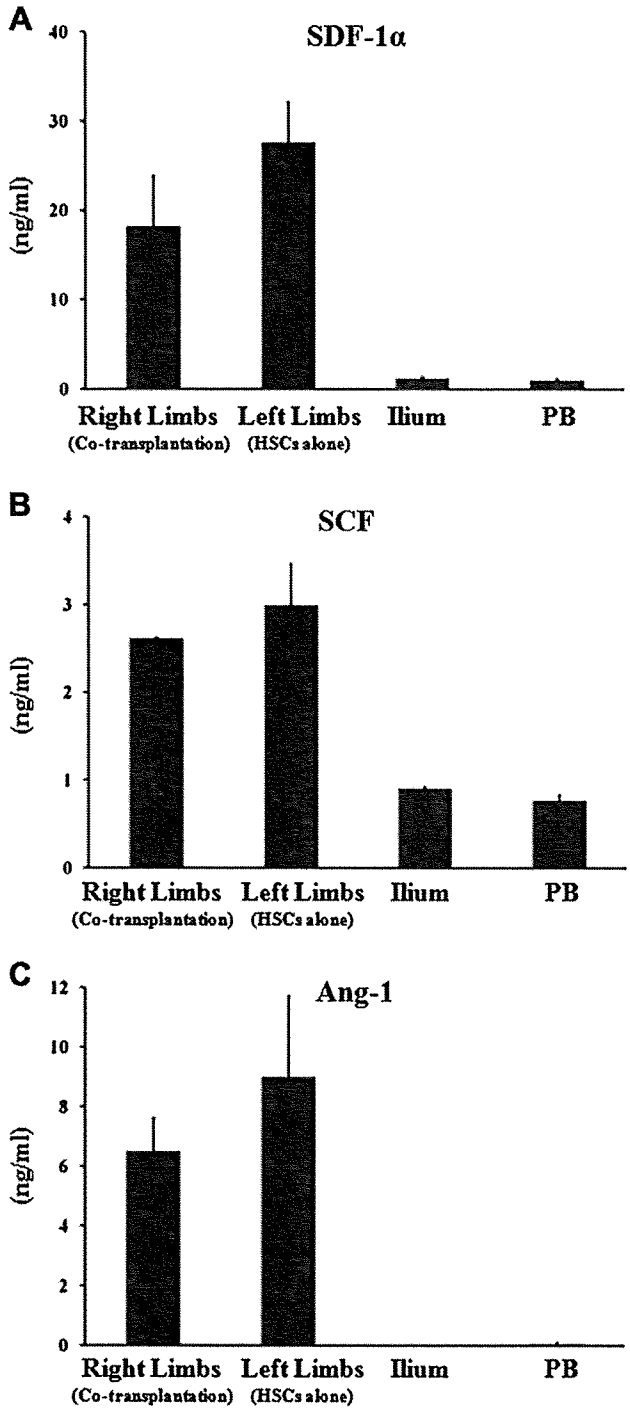

Supplemental Figure E1. Cytokine levels in the bone marrow (BM) and peripheral blood (PB) post intra-bone marrow transplantation. Stromal derived factor-1α (**A**), stem cell factor (**B**), and angiopoietin-1 (**C**) in the PB and BM plasma were quantified with enzyme-linked immunosorbent assay that was shown to cross-react with cynomolgus counterparts. The sample plasma was obtained from the limb marrow (humerus and femur of right or left side), ilium marrow, and PB in Monkey 3 on day 56 post-transplantation. The cytokine concentrations in the cotransplantation site (right side) and hematopoietic stem cells alone site (left side) are shown. The ilium is not an injection site and thus serves as controls. The PB also serves as controls. Data represent mean ± standard deviation.

THE JOURNAL OF GENE MEDICINE
J Gene Med 2009; 11: 373–381.
Published online 9 March 2009 in Wiley InterScience (www.interscience.wiley.com) **DOI:** 10.1002/jgm.1313

RESEARCH ARTICLE

Retroviral vector-producing mesenchymal stem cells for targeted suicide cancer gene therapy

Ryosuke Uchibori[1]
Takashi Okada[1†]
Takayuki Ito[1]
Masashi Urabe[1]
Hiroaki Mizukami[1]
Akihiro Kume[1]
Keiya Ozawa*[1]

[1]*Division of Genetic Therapeutics, Center for Molecular Medicine, Jichi Medical University, Tochigi, Japan*

*Correspondence to: Keiya Ozawa, Division of Genetic Therapeutics, Jichi Medical University, 3311-1 Yakushiji, Shimotsuke, Tochigi 329-0498, Japan.
E-mail: titou@jichi.ac.jp

†Present address: Department of Molecular Therapy, National Institute of Neuroscience, National Center of Neurology and Psychiatry, Tokyo, Japan.

Received: 30 May 2008
Revised: 31 October 2008
Accepted: 19 January 2009

Abstract

Background Mesenchymal stem cells (MSCs) are a promising vehicle for targeted cancer gene therapy because of their potential of tumor tropism. For efficient therapeutic application, we developed retroviral vector-producing MSCs that enhance tumor transduction via progeny vector production.

Methods Rat bone marrow-derived MSCs were nucleofected with the proviral plasmids (vesicular stomatitis virus-G protein-pseudotyped retroviral vector components) (VP-MSCs) or pLTR plasmid alone (non-VP-MSCs). The luciferase-based *in vivo* imaging system was used to assess gene expression periodically. To evaluate the anticancer effects, we administered MSCs expressing herpes simplex virus-thymidine kinase (HSV-*tk*) into the left ventricular cavity of nude mice engrafted with 9L glioma cells subcutaneously.

Results *In vivo* imaging revealed that administration of luciferase-expressing non-VP-MSCs enhanced the bioluminescence signal at the inoculation sites of 9L cells, whereas no accumulation was observed in mice at the site of the control Rat-1 fibroblasts. Compared to non-VP-MSCs, the administration of VP-MSCs resulted in significant augmentation of the signal with an increase in transgene copy number. Immunohistochemical analysis showed marked luciferase expression at the tumor periphery in mice injected with VP-MSCs, whereas little expression was detected in those injected with non-VP-MSCs. Under the continuous infusion of ganciclovir, systemic administration of VP-MSCs expressing HSV-*tk* suppressed tumor growth more effectively than non-VP-MSC administration, whereas no anticancer effect was observed without ganciclovir treatment. Furthermore, VP-MSC administration caused no transgene transduction in the normal tissues and organs.

Conclusions VP-MSCs accumulated at the site of tumors after intravascular injection in tumor-bearing mice, followed by *in situ* gene transfer to tumors without transduction of normal organs. When applied to the HSV-*tk*/ganciclovir suicide gene therapy, more efficient tumor growth suppression was observed using VP-MSCs compared to non-VP-MSCs. This VP-MSC-based system has great potential for improved cancer gene therapy. Copyright © 2009 John Wiley & Sons, Ltd.

Keywords HSV-*tk*; in vivo imaging; retroviral vector; suicide cancer gene therapy; vector-producing MSCs

Introduction

Tumor invasions and metastases are the principal causes of death in patients with cancer. However, current anticancer strategies are typically associated with high toxicity and modest success rates. Suicide gene therapy has been tested for the treatment of invasive tumors such as malignant glioma; for this

therapy, retroviral vectors expressing herpes simplex virus-thymidine kinase (HSV-*tk*) combined with treatment with the prodrug ganciclovir (GCV) have been developed [1]. However, this system still has two hurdles, namely, the transduction efficiency of tumors and immune responses generated against the vectors [2]. In addition, it is essential that the vector has a tumor tracking property to effectively attack invasive or metastatic lesions with minimal adverse effects [3].

Mesenchymal stem cells (MSCs), as derived from adult bone marrow, fat, or fetal tissues, are a promising tool for regenerative medicine because of their self-renewal capacity and multilineage differentiation ability. Recent evidence suggests that bone marrow-derived MSCs selectively accumulate at tumors, and they are promising vehicles for tumor-targeting therapy [4,5]. However, MSCs may provide structural support to malignant cells and locally attenuate the tumor surveillance system through their immunosuppressive effects, leading to the progression of tumor growth [6–8]. Therefore, MSCs should be modified to have an increased antitumor activity in order to use them for cancer gene therapy [5,9,10].

Systemic administration of genetically modified MSCs to produce an anticancer cytokine has been shown to be effective in tumor suppression. Intravenous injection of MSCs expressing interferon (IFN)-β inhibits the expansion of the pulmonary metastasis of melanoma and breast cancer in mice [11] and prolongs the survival of mice with glioma xenografts [4]. For more efficient and specific MSC-based gene therapy, we aimed to develop MSCs with a vector-producing property.

In the present study, we developed MSCs that locally produce the HSV-*tk*-expressing retroviral vectors (VP-MSCs), which facilitate transgene transduction and tumor targeting. By using a mouse subcutaneous glioma model, we examined tumor tropisms and cancer-killing effects of systemically administered VP-MSCs. To assess the safety of this system, we demonstrated that tumor-specific transduction was achieved by the progeny retroviruses produced by VP-MSCs at the site of tumors.

Materials and methods

Cell culture

The malignant rat glioma cell line 9L and fibroblasts derived from a normal rat Rat-1 were obtained from the Riken BRC Cell Bank (Ibaraki, Japan) [12]. The stable firefly luciferase-expressing rat MSCs and 9L (9L/LNCL) were developed by transduction with a recombinant retroviral vector encoding luciferase and neomycin resistance genes. The cells were cultured in Dulbecco's modified Eagle's medium and nutrient mixture F12 (DMEM-F12; Invitrogen, Grand Island, NY, USA) and 10% fetal bovine serum (FBS; Sigma Chemical Co., St Louis, MO, USA) supplemented with 100 units/ml of penicillin and 100 μg/ml of streptomycin in an atmosphere of 5% CO_2 at 37 °C.

MSC isolation and culture

All animal experiments were approved by the Jichi Medical University ethics committee and were performed in accordance with the National Institutes of Health Guide for the Care and Use of Laboratory Animals. MSCs were prepared from the rat bone marrow as described previously [13]. Briefly, 5-week-old male Sprague-Dawley (SD) rats (Clea Japan, Tokyo, Japan) were sacrificed by an overdose of isoflurane inhalation, and their femurs and tibias were dissected. After the epiphyses were removed, the bone marrow was flushed out with DMEM-F12. A single cell suspension was obtained by sequential drawing of the marrow into syringes through 27-G needles. The cells were cultured at a density of 1×10^6 cells/cm^2 in noncoated T-25 or T-75 cell culture flasks containing DMEM-F12 and 10% FBS supplemented with 100 units/ml of penicillin and 100 μg/ml of streptomycin in an atmosphere of 5% CO_2 at 37 °C. After 3 or 4 days of culture, the medium was replaced and the non-adherent cells removed. Thereafter, the medium was then changed twice weekly. When 60–80% confluence was attained, the adherent cells were placed at a density of 1×10^4 cells/cm^2 in a T-225 flask for expansion. After 15 passages, the cells were used for the experiments.

VP- and non-VP-MSC preparation

HSV-*tk* or the firefly luciferase expression cassette was cloned into pLTR to create pLTR-*tk* or pLTR-*luc*. pGP and pVSV-G express the Moloney murine leukemia virus gag-pol and the vesicular stomatitis virus-G (VSV-G) pseudotyped envelope protein under the control of a cytomegalovirus promoter, respectively [12]. Nucleofection of MSCs was performed according to the manufacturer's instructions (Amaxa Biosystem, Cologne, Germany). To generate VP-MSCs, 2×10^6 MSCs were gently resuspended in 100 μl of Human Mesenchymal Nucleofector Solution (Amaxa Biosystem) and mixed with the proviral plasmids pGP, pVSV-G and pLTR-*tk* or pLTR-*luc* at concentrations of 1, 1 and 2 μg, respectively. The mixture was then pulsed with the program U-23. Non-VP-MSCs were generated by nucleofection with pLTR-*tk* or pLTR-*luc* alone. Vector-producing HEK293 (VP-293) cells and non-VP-293 cells were similarly developed by nucleofection using the X-01 pulse program. Cells were cultured in six-well plates containing prewarmed DMEM-F12 before the experiments. Quantification of RNA genome titer in culture supernatant was determined by reverse transcription-quantitative polymerase chain reaction (PCR) using a Retrovirus Titer Set (Takara Bio Inc., Shiga, Japan) according to the manufacturer's instructions. The results of viral titer were expressed as genomes/μl.

DOI: 10.1002/jgm

Transduction of 9L cells and MSCs with progeny retrovirus produced by VP-MSCs

The 100-μl culture supernatants of luciferase-expressing VP-MSCs or non-VP-MSCs in a 96-well plate after 24 h of nucleofection were added to 9L cells or MSCs (1×10^4 cells for each well) in a 96-well plate. After 48 h of incubation, transduction efficiency was estimated by the luciferase assay using a chemiluminometer (Fluoroskan Ascent FL, Thermo Labsystem, Beverly, MA, USA) and the Bright-Glo Reagent kit (Promega, Madison, WI, USA) according to the manufacturer's instructions.

Chemiluminescence assay for evaluating tumor-killing effects *in vitro*

9L/LNCL cells stably expressing luciferase were used in the present study. Briefly, 5×10^4 9L/LNCL cells were cocultured with 2.5×10^4 VP-MSCs or non-VP-MSCs in 48-well flat-bottomed plates (day 0). At day 3, the cells were exposed to varying concentrations (0.01–100 μmol/l) of GCV (F. Hoffmann-La Roche, Basel, Switzerland). At day 7, the luciferase assay was performed with a chemiluminometer (Thermo Labsystem) using the Bright-Glo Reagent kit (Promega) according to the manufacturer's instructions.

Determination of HSV-tk transgene copy number *in vitro*

To estimate the copy number of transgene in the cells transduced with retroviral progeny, 9L cells and MSCs were co-cultured and whole cells were collected at day 7. Quantitative values were obtained from the threshold cycle (Ct) number that indicated exponential amplification of the PCR product by using a sequence detection system (ABI Prism 7700; Applied Biosystems, Madison, WI, USA). The relative copy number of the HSV-*tk* gene was determined as the ratio of the copy numbers in the group of 9L cells co-cultured with VP-MSCs to the copy numbers in the non-VP-MSC group. The copy number of the reference gene *GAPDH* was also determined to correct the variation in the DNA amount and amplification efficiency. The gene specific primers are shown below: HSV-*tk* forward, 5′-CGTCGCCGATGGGGTGTTCT-3′, reverse, 5′-GCGCGGCCGGGTAGCACAGG-3′, rat *GAPDH* forward, 5′-CAGCAATGCATCCTGCAC-3′, and reverse, 5′-GAGTTGCTGTTGAAGTCACAGG-3′.

In vivo bioluminescence imaging for detecting transgene expression

9L cells or Rat-1 cells (3×10^6 each) in 100 μl of phosphate buffer saline (PBS) containing 25% (v/v) basement membrane matrix (Matrigel; BD Biosciences, Franklin Lakes, NJ, USA) were subcutaneously inoculated into the bilateral dorsal region (3×10^6 cells/site) of 4- to 6-week-old male Balb/c nu/nu mice (Clea Japan). Immediately after inoculation, the luciferase-expressing VP-MSCs or non-VP-MSCs (5×10^5 cells/body each) were injected into the left ventricular cavity of mice. Three experimental groups were formed: group 1, mice inoculated with Rat-1 cells and injected with non-VP-MSCs; group 2, mice inoculated with 9L cells and injected with non-VP-MSCs; and group 3, mice inoculated with 9L cells and injected with VP-MSCs; $n = 4$ for each group. After injection of the cells, optical bioluminescence imaging was performed to periodically trace the cells using an *in vivo* imaging system (IVIS; Xenogen, Hopkinton, MA, USA). The reporter substrate D-luciferin (75 mg/kg body weight) was injected into the mouse peritoneum for scanning. The luminescence levels in the region of interest (total flux; photons/sec) were analysed using the Living Image software (Xenogen, Alameda, CA, USA).

Immunohistochemistry

Mice were anesthetized with an overdose of isoflurane inhalation and fixed by perfusion with 4% paraformaldehyde. The tissues were then embedded in an optimal cutting temperature compound (Sakura Finetek, Tokyo, Japan), frozen, and sectioned into 20-μm-thick slices. Immunohistochemical staining was performed with a rabbit monoclonal anti-luciferase antibody (1 : 5000; Promega) by the avidin-biotin-peroxidase method. Irrelevant rabbit immunoglobulin (Ig)G (Promega) was used as a negative control. Sections were treated with horseradish peroxidase-labelled anti-rabbit IgG secondary antibody (Dako, Glostrup, Denmark; 1 : 200), and luciferase-positive cells were visualized using the Vectastain Elite ABC kit (Vector Laboratories, Burlingame, CA, USA). The sections were counterstained with hematoxylin.

Determination of luciferase transgene copy number *in vivo*

To estimate the copy number of transgene in tissues in tumor-bearing mice, small pieces of tissues were obtained from peripheral and central portions of the tumors at 21 days after MSC administration. Quantitative values were obtained from the threshold cycle (Ct) number that indicated exponential amplification of the PCR product by using the sequence detection system (ABI Prism 7700). The relative copy number of the *luciferase* gene was determined as the ratio of the copy numbers in the peripheral or central portions of tumors in the group of 9L tumor in mice inoculated with VP-MSCs to the copy numbers in non-VP-MSCs group. The copy number of the reference gene *GAPDH* was also determined to correct for variation in the DNA amount

DOI: 10.1002/jgm

and amplification efficiency. The gene specific primers were: *Luc* forward, 5′-TTCTGGGGGCGCACCTCTTC-3′, and reverse, 5′-GGGGGCCACCTGATATCCTTTGTA-3′.

Survival of MSCs at the tumor sites *in vivo*

The stable luciferase-expressing MSCs were mixed with an equal number of nontransduced 9L cells (1.5×10^6 cells each) and were suspended in 100 μl of PBS containing 25% (v/v) Matrigel. Immediately, the mixture was subcutaneously inoculated into the bilateral dorsal region of nu/nu mice ($n = 4$ for each group). Luminescence at the tumor sites was periodically determined using IVIS (Xenogen), and the luminescence levels were analysed using Living Image software (Xenogen).

Assessment of tumor-specific transduction

To estimate the level of progeny retroviral transduction, PCR analysis was performed. DNA was extracted from the tumors or normal tissues by using a DNA extraction kit (Qiagen) at 21 days after MSC injection and then amplified using Ex Taq (Takara Bio Inc.). The PCR products (560 bp) extending from the 5′ long-terminal repeat (LTR) or 3′-LTR of the retroviral vector were produced using the gene-specific primers: LTR forward, 5′-AGGGCCAAGAACAGATGAGACAGC-3′ and reverse, 5′-GTACAGACGCAGGCGCATAACATC-3′. Conversion of the 3′-LTR to the 5′-LTR after retroviral transduction was confirmed by the typical banding pattern (440 bp + 120 bp fragments) generated after *Xba*I digestion.

Assessment of the anticancer effects of VP-MSCs *in vivo*

9L/LNCL cells (3×10^6 each) in 100 μl of PBS containing 25% (v/v) Matrigel were subcutaneously inoculated in the bilateral dorsal region of 4- to 6-week-old male Balb/c nu/nu mice. PBS (group 1), MSCs (group 2), HSV-tk-expressing non-VP-MSCs (group 3) or VP-MSCs (group 4; 5×10^5 cells/body each) were then injected into the left ventricular cavity of the mice ($n = 4$ for each group). Seven days after MSC injection, GCV (100 mg/kg/day) or PBS was continuously administered into the peritoneum by using mini-osmotic pumps (Alzet, Palo Alto, CA, USA) for 28 days. The tumor growth was monitored two or three times a week by measuring tumor sizes using a caliper, and tumor volumes were calculated using the formula: tumor volume (mm^3) = $a(mm) \times b^2(mm^2) \times 0.5$ (a, the height of the tumor; b, the width of the tumor).

Statistical analysis

Data from multiple experiments are expressed as the mean ± SEM. Statistical analyses were performed using StatView (Abacus Concepts, Inc., London, UK). Differences in parameters were evaluated by analysis of variance combined with Welch's t-test. $p < 0.05$ was considered statistically significant.

Results

Characterization of VP-MSCs

Consistent with previous studies, the bone marrow-derived rat MSCs used in the present study exhibited a spindle shape; they differentiated into adipocytes, osteocytes, and chondrocytes in appropriate culture media (data not shown). The green fluorescence protein (GFP)-based semiquantitative analysis revealed that nucleofection is more efficient for the transfection of MSCs than the calcium-phosphate method and lipofection: the percentage of GFP-positive MSCs after 24 h of transfection by each method was approximately 60.1%, 3.1% and 12.3%, respectively.

The secretion of retroviral vectors into the culture media of VP-MSCs (Figure 1a) and VP-293 cells (Figure 1b) increased and peaked at 48 h after nucleofection, whereas the vector production from non-VP-MSCs or non-VP-293 cells was undetectable. There was no significant difference in the amounts of produced vectors at 48 h between VP-MSCs and VP-293 cells.

Chemiluminescence assay showed that 9L glioma cells were efficiently transduced with the vectors generated from VP-MSCs (Figure 1c). On the other hand, when MSCs were treated with the culture media of VP-MSCs or non-VP-MSCs, transduction was undetectable (Figure 1d).

Tumor-killing effects of VP-MSCs *in vitro*

The *in vitro* luciferase assay revealed that the bioluminescence signal of luciferase-expressing 9L/LNCL cells decreased in a GCV dose-dependent manner after coculture with HSV-*tk*-expressing MSCs (Figure 1e). The concentration required to induce a 50% inhibition (IC_{50}) value of GCV in the presence of VP-MSCs at day 7 was considerably lower than that in the presence of non-VP-MSCs (0.33μmol/l versus 83μmol/l). At this time-point, real-time PCR analysis showed that the relative copy number of the HSV-*tk* gene in the VP-MSC group was approximately 17.5-fold more than that in the non-VP-MSC group (Table 1). Because transduction of MSCs with progeny retrovirus was inefficient (Figure 1d), these data suggests that 9L glioma cells were mainly transduced with progeny luciferase-expressing retrovirus produced by VP-MSCs (Figure 1c).

DOI: 10.1002/jgm

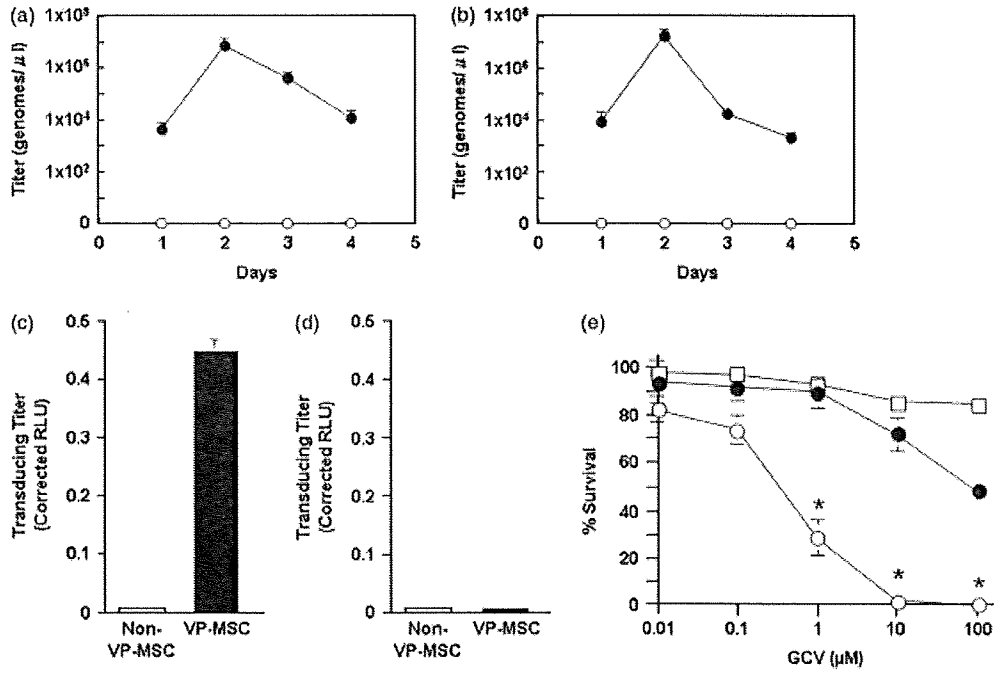

Figure 1. Function of vector-producing mesenchymal stem cells (VP-MSCs) *in vitro*. (a, b) Time course of luciferase-expressing retrovirus production from VP-MSCs and vector-producing HEK293 (VP-293) cells. VP-MSCs (a, ●; $n = 3$) or VP-293 (b, ●; $n = 3$) were developed with pGP, pVSV-G, and pLTR-*luc* at concentrations of 1, 1 and 2 μg by nucleofection. Non-VP-MSCs (a, ○; $n = 3$) or non-VP-293 (b, ○; $n = 3$) were developed with pLTR-*luc* by nucleofection. The RNA genome titer of progeny virus in the culture supernatant of these cells was determined by reverse transcription-quantitative PCR. (c, d) Transduction of rat glioma 9L cells (c) or MSCs (d) with luciferase-expressing retrovirus produced by VP-MSCs. The 9L cells and MSCs were treated with the culture supernatant of non-VP-MSCs (open bar; $n = 3$) or VP-MSCs (solid bar; $n = 3$) that were nucleofected 2 days before. The luminescence levels of these cells were measured by a chemiluminescence luciferase assay after 48 h of treatment. (e) Tumor-killing effects of VP-MSCs *in vitro*. MSCs were cocultured with luciferase-expressing 9L/LNCL glioma cells at a ratio of 1 : 3 (day 0), and different doses of GCV (0.01–100 mmol/l) were added to the culture media on day 3. The number of viable 9L/LNCL cells was estimated by a luciferase assay on day 7. The groups were as follows: MSCs without genetic modification (□); MSCs nucleofected with herpes simplex virus-thymidine kinase (HSV-*tk*)-expressing plasmid (non-VP-MSCs, ●); and MSCs nucleofected with retroviral vector components pLTR-*tk*, pGag-pol, and pVSV-G (VP-MSCs, ○). For each group, $n = 3$; $^*p < 0.05$ versus non-VP-MSC group

Table 1. Relative HSV-*tk* transgene copy number in the co-cultures of 9L tumor cells and MSCs

	Relative HSV-*tk* transgene copy number
Non-VP-MSCs	1.0
VP-MSCs	17.5

9L cells and MSCs were co-cultured and whole cells were collected at day 7. The relative copy number of the HSV-*tk* gene was determined as the ratio of the copy numbers in the group of 9L cells co-cultured with VP-MSCs to the copy numbers in the non-VP-MSC group. The copy number of the reference gene *GAPDH* was also determined to correct the variation in the DNA amount and amplification efficiency.

Tumor tropism of VP-MSCs *in vivo* and enhanced transgene expression *in situ*

In vivo imaging indicated that luciferase-expressing MSCs transiently appeared just after injection at high perfusion organs, such as the brain, liver, kidney and spleen, irrespective of administration of VP- or non-VP-MSCs (day 0). After systemic administration of non-VP-MSC, the signal peaked at day 10 and declined thereafter at the tumor sites, whereas no signal enhancement was observed at the site of Rat-1 inoculation (Figures 2a and 2b). By contrast, the signal after administration of VP-MSCs further increased over day 21 (Figures 2c and 2d), and no signal was observed in the normal organs at this time-point. Immunohistochemical studies showed marked luciferase expression at the tumor periphery in the VP-MSC group after 21 days of administration (Figure 2e). No signal of luciferase expression was observed in the normal tissues at this time-point. Real-time PCR analysis revealed that the relative copy number of the luciferase gene at the tumor periphery of the VP-MSC group was approximately 47.5-fold more than that of the non-VP-MSC group (Table 2). These results indicate not only successful retroviral vector production by VP-MSCs, but also effective gene transfer by progeny retrovirus *in situ*.

Survival of MSCs at the tumor site

The enhanced signal observed in the VP-MSC group may be in part due to expansion or division of VP-MSCs *in situ*. To exclude this possibility, we estimated the survival of MSCs in the vicinity of the 9L tumor. We employed stable luciferase-expressing MSCs to avoid the conditions of transient gene expression. When the cells were inoculated with 9L tumor cells at the dorsal region

DOI: 10.1002/jgm

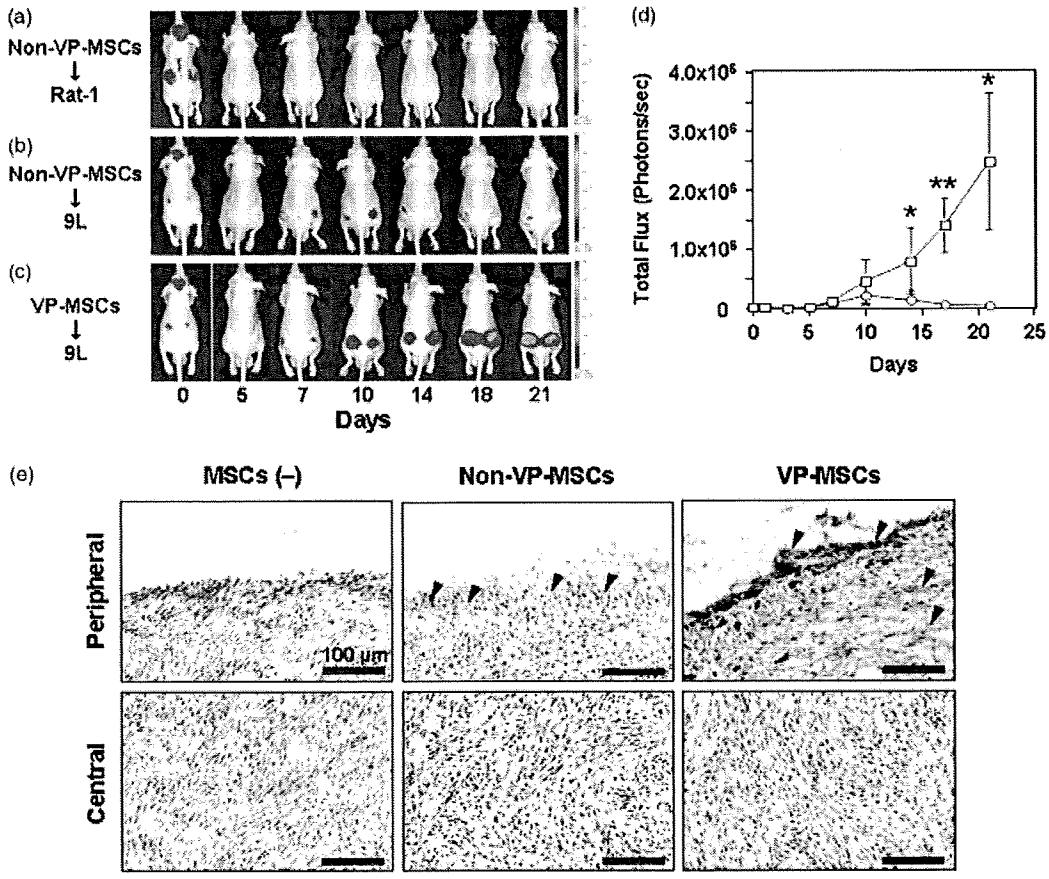

Figure 2. Tumor tropism and enhanced transgene expression after VP-MSC administration. Rat-1 fibroblasts (a) or 9L glioma cells (b, c) were subcutaneously inoculated into the bilateral dorsal region of Balb/c nu/nu mice (3×10^6 cells/site). Luciferase-expressing MSCs (5×10^5 cells/body) were then administered through the left ventricular cavity (day 0). Luminescence was periodically measured through an intraperitoneal injection of D-luciferin (days 0–21). (d) Quantification of luminescence levels at the 9L tumor site after injection of VP-MSCs (□) or non-VP-MSCs (○). For each group, $n = 4$; $^*p < 0.05$ or $^{**}p < 0.01$ versus non-VP-MSC group. (e) Immunostaining for luciferase expression in the subcutaneous tumor. MSCs (5×10^5 cells/body) were injected into the left ventricular cavity immediately after subcutaneous inoculation of 9L cells in the bilateral dorsal part of the Balb/c nu/nu mice (day 0). The tumor tissues were obtained 21 days after MSC administration. Luciferase-positive cells (brown) were detected at the tumor periphery with an anti-luciferase antibody. Arrowheads, luciferase-positive cells. Scale bar = 100 mm

Table 2. Relative *luciferase* transgene copy number in 9L tumors in mice inoculated with VP-MSCs

		Relative *luciferase* transgene copy number	
		Experiment 1	Experiment 2
Central	Non-VP-MSCs.Luc	ND	ND
	VP-MSCs.Luc	ND	ND
Peripeheral	Non-VP-MSCs.Luc	1.0	1.0
	VP-MSCs.Luc	47.5	27.7

Small pieces of tissues were obtained from peripheral and central portions of tumors at 21 days after MSC administration. The relative copy number of the *luciferase* gene was determined as the ratio of the copy numbers in the peripheral portions of tumor in the group of 9L tumors inoculated with VP-MSCs to the copy numbers in non-VP-MSCs. The copy number of the reference gene *GAPDH* was also determined to correct for variation in the DNA amount and amplification efficiency.

of the mice (day 0), the luciferase expression peaked at day 10 and rapidly declined after day 14 (Figures 3a and 3b), indicating the elimination of inoculated MSCs. These results suggest that the signal enhancement after day 14 in the VP-MSC group was not caused by the expansion of inoculated MSCs.

Tumor-specific transduction by VP-MSCs

We evaluated the progeny retroviral transuduction of the tissues at 21 days after MSC administration. The 5′-LTR sequence of transgene in VP-MSCs and non-VP-MSCs does not contain the *Xba*I site (Figure 4a, upper panel). On the other hand, the 5′-LTR sequence of transgene in target cells transduced with progeny retrovirus produced from VP-MSCs contains the *Xba*I site because this 5′-LTR is the copy of 3′-LTR (containing the *Xba*I site) in retroviruses (Figure 4a, lower panel). Therefore, the presence of two fragments (440 bp + 120 bp) of PCR products from the 5′-LTR region (560 bp) indicates that retroviral vector-mediated gene transfer occurred. Because the PCR products from the tumors in the VP-MSC group were digested into two fragments with *Xba*I (Figure 4b), ths means that the tumors were transduced with progeny

DOI: 10.1002/jgm